Provided for non-commercial research and education use.
Not for reproduction, distribution or commercial use.

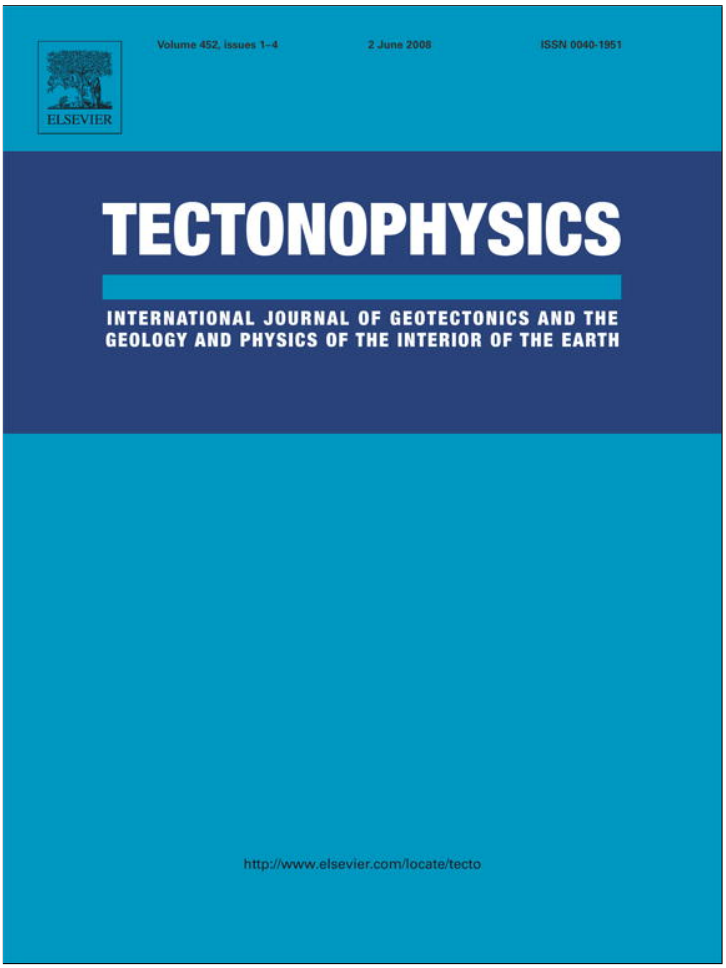

This article appeared in a journal published by Elsevier. The attached copy is furnished to the author for internal non-commercial research and education use, including for instruction at the authors institution and sharing with colleagues.

Other uses, including reproduction and distribution, or selling or licensing copies, or posting to personal, institutional or third party websites are prohibited.

In most cases authors are permitted to post their version of the article (e.g. in Word or Tex form) to their personal website or institutional repository. Authors requiring further information regarding Elsevier's archiving and manuscript policies are encouraged to visit:

http://www.elsevier.com/copyright

Author's personal copy

Tectonophysics 452 (2008) 51–65

Contents lists available at ScienceDirect

Tectonophysics

journal homepage: www.elsevier.com/locate/tecto

The April 2007 earthquake swarm near Lake Trichonis and implications for active tectonics in western Greece

A. Kiratzi [a,*], E. Sokos [b], A. Ganas [c], A. Tselentis [b], C. Benetatos [a], Z. Roumelioti [a], A. Serpetsidaki [b], G. Andriopoulos [b], O. Galanis [a], P. Petrou [c]

[a] Department of Geophysics, Aristotle University of Thessaloniki, 54124 Thessaloniki, Greece
[b] Seismological Laboratory, University of Patras, Rio 261 10, Greece
[c] National Observatory of Athens, Geodynamic Institute, 11810 Athens, Greece

ARTICLE INFO

Article history:
Received 18 September 2007
Received in revised form 4 February 2008
Accepted 14 February 2008
Available online 4 March 2008

Keywords:
Lake Trichonis
Western Greece
Focal mechanisms
Strike-slip
Earthquake
Tectonics

ABSTRACT

We investigate the properties of the April 2007 earthquake swarm (Mw 5.2) which occurred at the vicinity of Lake Trichonis (western Greece). First we relocated the earthquakes, using P- and S-wave arrivals to the stations of the Hellenic Unified Seismic Network (HUSN), and then we applied moment tensor inversion to regional broad-band waveforms to obtain the focal mechanisms of the strongest events of the 2007 swarm. The relocated epicentres, cluster along the eastern banks of the lake, and follow a distinct NNW–ESE trend. The previous strong sequence close to Lake Trichonis occurred in June–December 1975. We applied teleseismic body waveform inversion, to obtain the focal mechanism solution of the strongest earthquake of this sequence, i.e. the 31 December 1975 (Mw 6.0) event. Our results indicate that: a) the 31 December 1975 Mw 6.0 event was produced by a NW–SE normal fault, dipping to the NE, with considerable sinistral strike-slip component; we relocated its epicentre: i) using phase data reported to ISC and its coordinates are 38.486°N, 21.661°E; ii) using the available macroseismic data, and the coordinates of the macroseismic epicentre are 38.49°N, 21.63°E, close to the strongly affected village of Kato Makrinou; b) the earthquakes of the 2007 swarm indicate a NNW–SSE strike for the activated main structure, parallel to the eastern banks of Lake Trichonis, dipping to the NE and characterized by mainly normal faulting, occasionally combined with sinistral strike-slip component. The 2007 earthquake swarm did not rupture the well documented E–W striking Trichonis normal fault that bounds the southern flank of the lake, but on the contrary it is due to rupture of a NW–SE normal fault that strikes at a ~45° angle to the Trichonis fault. The left-lateral component of faulting is mapped for the first time to the north of the Gulf of Patras which was previously regarded as the boundary for strike-slip motions in western Greece. This result signifies the importance of further investigations to unravel in detail the tectonics of this region.

© 2008 Elsevier B.V. All rights reserved.

1. Introduction

On 8 April 2007 an earthquake swarm burst near the SE bank of Lake Trichonis, a lake overlying the Trichonis graben in western Greece. The three strongest events of the swarm occurred on April 10th at 03:17, 07:15 and 10:41 GMT with moderate magnitudes ranging from Mw 5.0 to Mw 5.2. The most serious damage was reported in the village Thermon 5 km to the NE of the earthquake epicentres. Lake Trichonis, located to the east of the city of Agrinio and to the north of the cities of Nafpaktos and Messolongi, is the largest natural lake in Greece, with surface area of 97 km^2, a maximum water depth of 58 m and an approximate water volume of 2.8×10^9 m^3 (Zacharias et al., 2005). The lake itself constitutes a significant ecosystem.

Fig. 1 summarizes the historical (before 1911 for Greece) and instrumental seismicity with Mw≥6.0, together with the Mw≥4.0 seismicity as relocated by Roumelioti et al. (2007), and the focal mechanisms of the strongest previous events from the database of Kiratzi and Louvari (2003) and Kiratzi et al. (2007). It is clearly seen that Lake Trichonis and its immediate vicinity have never been the site of frequent strong earthquakes (Ambraseys, 2001a,b; Papazachos and Papazachou, 2003). The seismicity is sparse and the strongest event registered for the region occurred in 1975. However by looking closely, a concentration of epicentres around the south-east area of Lake Trichonis is observed. In the past, the city of Agrinio, at the northwestern bank of the lake, was severely affected by the occurrence of an intermediate depth event (not shown in Fig. 1) on 31 March 1965 (GMT 09:47:31, 38.6°N, 22.4°E, h=78 km, M=6.8, Io=VIII+ in Agrinio), whereas the city of Nafpaktos was mostly affected by the 24 December 1917 event (GMT 09:13:55; 38.4° N, 21.7° E; h=n, M=6.0, Io=VIII in Nafpaktos; Papazachos and Papazachou, 2003).

In this study, we first revisit the strongest 1975 events, in order to relocate them, invert for the focal mechanism using teleseismic recordings and search for evidence for the fault plane; then, we study the 2007 swarm using regional digital broad-band records to calculate

* Corresponding author. Tel.: +30 2310 998486; fax: +30 2310 998528.
E-mail address: Kiratzi@geo.auth.gr (A. Kiratzi).

0040-1951/$ – see front matter © 2008 Elsevier B.V. All rights reserved.
doi:10.1016/j.tecto.2008.02.009

Author's personal copy

Fig. 1. The Trichonis Lake as located in the broader Aitolia-Akarnania region. Historical (before 1911 for Greece) and instrumentally recorded strong (Mw>6.0) events are shown (large encircled asterisks; dates and magnitudes are also shown) together with the Mw>4.0 instrumental seismicity (small asterisks). (Source of historical information: Ambraseys, 2001a,b; Papazachos and Papazachou, 2003); (source of instrumental seismicity: Roumelioti et al., 2007; and the on-line catalogue of the University of Thessaloniki, Dept of Geophysics). (Source of plotted focal mechanisms: from Kiratzi and Louvari, 2003; Kiratzi et al., 2007 and references therein). The faults are from Doutsos et al. (1987), Lekkas and Papanikolaou (1997) and Goldsworthy et al. (2002). The sinistral strike-slip faults (black lines and arrows), that connect the Gulf of Amvrakikos and the Gulf of Patras, form the Amphiloxia–Katouna–Aitoliko Fault Zone, representing a subsiding basin. (The topography in all our maps was produced using Shuttle Radar Topography Mission (SRTM 3 arc — 30 m) data, available through NASA).

the focal mechanisms of the strongest events, relocate epicentres and discuss the results in view of the general tectonics of the region.

2. Tectonic setting

The Trichonis graben (Fig. 1) is a well-known Quaternary structure of western Greece that strikes WNW–ESE for a distance of about 32 km (between the villages of Angelokastron and Kato Makrinou) and has a width of about 10 km (Doutsos et al., 1987). The graben cuts across the early Tertiary NW–SE fold and thrust structures of the Pindos Mountains and strikes almost parallel to the Gulf of Patras graben about 30 km to the south (Brooks and Ferentinos 1984; Doutsos et al., 1988; Melis et al., 1989; Kokkalas et al., 2006). The regional geology comprises formations of the Pindos and Gavrovo isopic zones of the External Hellenides, mainly consisting of carbonates and flysch. The bedrock is extensively folded with long, anticline ridges extending as much as 6 km near the village Thermon. The thrust vergence is to the west. The orientation of the Trichonis graben, the high elevation of the footwall block (near 900 m) and the formation of a small sedimentary basin indicate on-going, north–south extension of the crust, also indicated by the focal mechanisms of moderate magnitude earthquakes (Hatzfeld et al., 1995; Kiratzi and Louvari, 2003). The Trichonis fault is the major, topography controlling normal fault, is north-dipping and bounds the south shore of the lake (Doutsos et al., 1987) where it is locally buried under Pleistocene deposits and thick alluvial cones. The fault forms a distinct topographic escarpment with clear drainage incision in the footwall block. For most part the fault uplifts folded Miocene flysch deposits and Eocene limestone in its footwall (British Petroleum Co. Ltd, 1971), but to the west (Lake Lysimachia area) the fault steps northwards, uplifting young lacustrine sediments in its footwall. The topography along the north shore of the lake is less pronounced pointing to the existence of a less active margin in comparison to the south.

Goldsworthy et al. (2002) report geomorphological evidence for the relative young age of the Trichonis fault. An old drainage course is preserved in the footwall block of the main fault, forming a steep and deep gorge (Kleisoura). As Goldsworthy et al. (2002) point out the gorge was excavated by a river that in the past flowed south from Panaitolikon Mountains towards the Gulf of Patras. It is important to note that now the gorge is abandoned and the drainage is diverted to

Author's personal copy

Table 1
Parameters (here determined or previously published) for the June – December 1975 events

Year	Month	Day	h:min:s	Lat °N	Lon °E	Depth	Mw	Nodal plane 1			Nodal plane 2			*P* axis		*T* axis		Reference
						km		Strike °	Dip °	Rake °	Strike °	Dip °	Rake °	az °	pl °	az °	pl °	
1975	06	30	13:26:55.3	38.466	21.641	4.4	5.6											This work – epicentre relocated with Hypoinverse using ISC phases
				38.481	21.671	–	5.6±0.17	112°±16° (or 292°)										This work – parameters determined using macroseismic data
				38.4	21.7	–	5.4 Ms											National Observatory of Athens (NOA) bulletins
				38.539	21.645	11	5.4 ML											NEIS
				38.489	21.623	3.1	5.0 mb											ISC
				38.48	21.63	–	5.7											Macroseismic epicentre (Papazachos et al., 1997)
1975	12	21	16:07:52.40	38.42	21.71	–	5.5	352	46	−54	126	54	−121	337	65	238	4	Focal mechanism with P-wave first motions (SP data) (Delibasis and Carydis, 1977)
1975	12	31	09:45:45.55	38.486	21.661	4+2/−2	6.0	316+5/−10	71+10/−20	−26+10/−10	55	66	−159	274	31	6	3	This work – epicentre relocated with Hypoinverse – depth and mechanism from teleseismic waveform modelling
				38.489	21.632	–	5.9±0.14	137°±34° (or 317°)	n/a									This work –parameters determined using macroseismic data
				38.5	21.7	–	5.9 Ms	236	39	−125	98	59	−65	55	66	170	11	National Observatory of Athens (NOA) bulletins and Papazachos (1975)
				38.63	21.80	19	5.5 Ms											NEIS
				38.524	21.673	15	5.5 Ms											ISC
				38.51	21.61	9	5.7											Macroseismic epicentre (Papazachos et al., 1997)

Author's personal copy

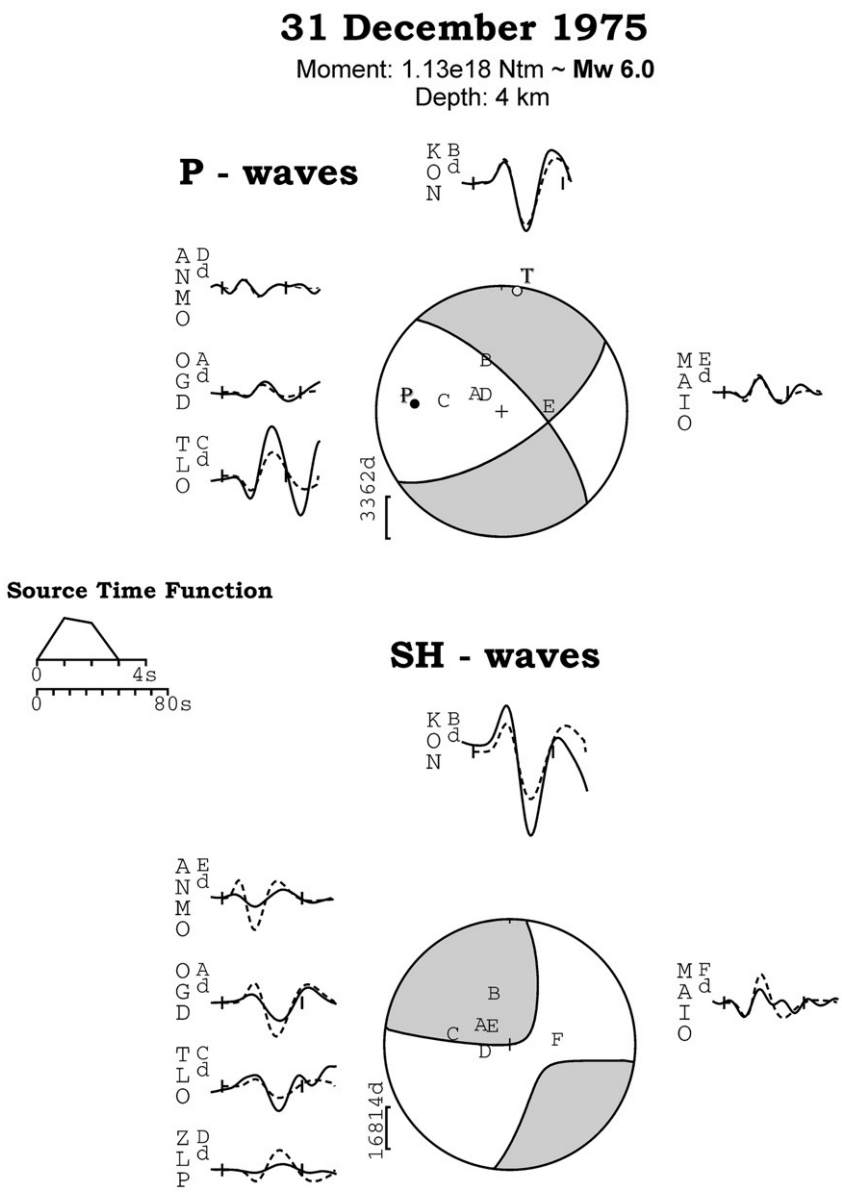

Fig. 2. Minimum misfit solution for the 31 December 1975 (the strongest instrumentally recorded event close to the 2007 swarm) calculated by inverting P and SH body waves for a point source, in a half-space of V_p=6.5 km/s, V_s=3.7 km/s and ρ=2.8 g/cm^3. The focal spheres show P (top) and SH (bottom) nodal planes in lower hemisphere projections; Observed (solid) and synthetic (dashed) waveforms are plotted around the focal spheres; the inversion window is indicated by vertical ticks, station codes are written vertically and station positions denoted by capital letters. The STF is the source time function, and the scale bar below it (in s) is that of the waveforms. *P* and *T* axes are also marked.

the west, and its flow is reversed, as it now flows to the north. It is therefore reasonable to assume that it is the late Quaternary footwall uplift of the Trichonis fault that has affected the whole process.

It is generally observed that during the 6 month period of April to September, 40% of the total annual outflows of the Trichonis Lake are pumped for agricultural purposes which results in very rapid water level drops more than 60 cm (mainly May–September) causing extended drought in the wetland area (Zacharias et al., 2005). It is of interest to note that both, the 1975 sequence and the 2007 swarm occurred within this period, but this is mainly a qualitative observation at this point.

3. The June–December 1975 sequence

3.1. Teleseismic waveform modelling of the 31 December 1975 event

The June–December 1975 seismic sequence is the most recent instrumentally recorded near the southern flank of Lake Trichonis. Two were the strongest events of the sequence, (Table 1 for parameters) which occurred on 30 June (Mw 5.6) and 31 December 1975 (Mw 6.0). The last event was preceded on 21 December 1975 by another strong (Mw 5.5) event, which occurred farther to the south of the activated region (Fig. 5). It was the 31 December event that produced landslides (Papadopoulos and Plessa, 2000) considerable structural damage at Kato Makrinou (200 old houses destroyed and 580 seriously cracked); one death and two injuries (Io=VIII–IX at Kato Makrinou; National Observatory of Athens (NOA) bulletins).

The focal mechanisms of the two strongest events of the region are significant for this study and the search at the IRIS depository for both events provided a number of good signal/noise waveforms for only the 31 December 1975 event. The 30 June 1975 event, had noisy records, and a teleseismic focal mechanism determination was not possible. A first motion polarity solution was not feasible either, due to insufficient data reported at IRIS.

For the 31 December 1975 event we retrieved 5 P and 6 SH waveforms with good signal/noise ratio from stations in teleseismic (30°

Author's personal copy

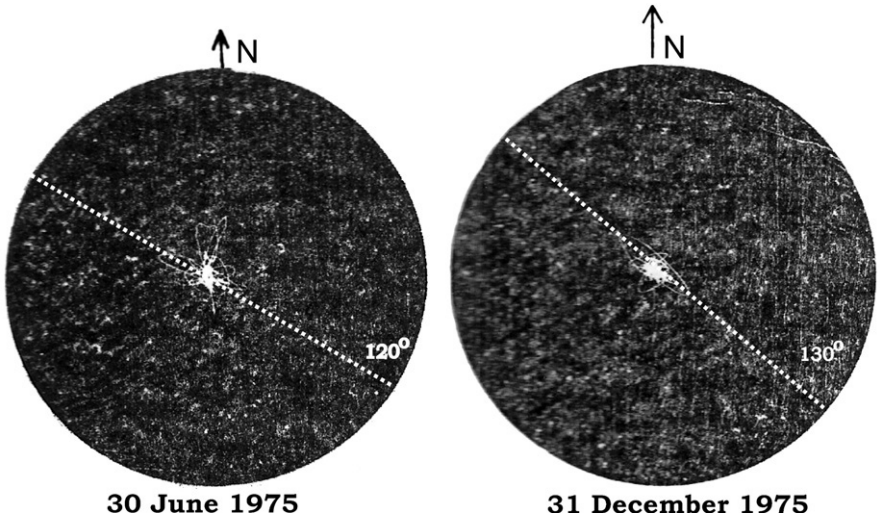

Fig. 3. Seismoscope (SR-100 Wilmot) records for the 30 June 1975 (left) and the 31 December 1975 (right) events obtained at Messolongi (Fig. 1 for location) ~24 km to the SW of the June–December 1975 epicentres. The records shown are those as included in the National Observatory of Athens (NOA) monthly bulletins. The 30 June 1975 caused a deflection of 13.6 mm in the N120°E direction and the 31 December 1975 event caused a deflection of 13.5 mm at ~N130°E (Person, 1977).

to 90°) distances. We used the MT5 software (Zwick et al., 1994) and the analysis procedures as described in detail elsewhere (e.g. Kiratzi and Louvari, 2003; Benetatos et al., 2004, 2005 and references therein) to invert for the focal mechanism parameters (strike/dip/rake), centroid depth and seismic moment, assuming a source represented as a point in space and described in time by a source time function consisting of overlapping isosceles triangles. Prior to the inversion waveforms have been filtered between 0.01 and 0.1 Hz and convolved with a typical WWSSN 15–100 s long-period instrument response. Green's functions have been calculated using a half-space of 6.5 km/s and 3.7 km/s for P-waves and S-waves, respectively and a density of 2.8 g/cm^3.

The best fitting solution (known as "the minimum misfit solution"), obtained after many test inversions, (Table 1 and Fig. 2) indicates normal faulting with a considerable strike-slip component. The simple-shape source time function has a total duration of 3 s. The solution obtained from waveform modelling, is in accordance with the mechanism

Fig. 4. Location of the broad-band stations (stars) of the Hellenic Unified Seismograph Network (HUSN), whose records were used in the relocation of epicentres (all stations were used) and the focal mechanism determination (station names underlined).

Author's personal copy

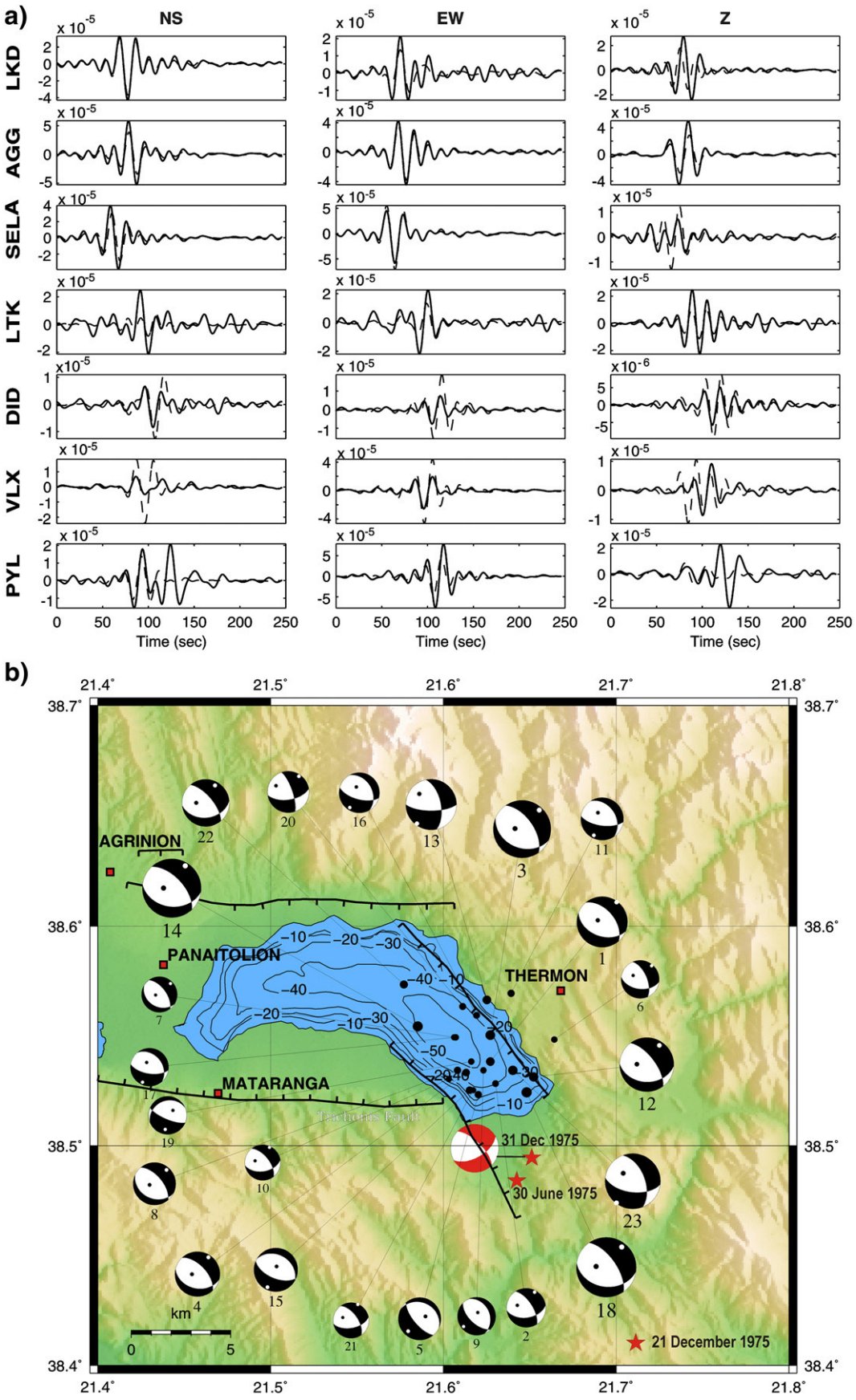

Fig. 5. a) Waveform fit between observed (solid line) and synthetic waveforms (dashed line) for event no. 14 in Table 2. Displacement waveforms are presented and amplitude scale is in meters. b) Focal mechanisms for twenty-three events of the 2007 swarm determined using regional moment tensor inversion (see Table 2 for parameters). Normal faulting along NNW–SSE trending planes is observed combined with strike-slip motions, for two events of the sequence pure strike-slip motions are observed. The 1975 epicentres and the mechanism for the 31 December 1975 event are included for comparison.

Author's personal copy

Table 2
Source parameters for the strongest 2007 events determined from regional moment tensor inversion (ISOLA code — see text for details); Q = quality of the solution based on the% of variance reduction, VR, with thresholds set at VR<40%, 60%<VR 40%, VR 60% for Q = C, B, A respectively; DC = double-couple percentage, CLVD = compensated linear vector dipole percentage; all locations are obtained by HypoDD except for events 18, and 23 which were obtained from Hypoinverse

No.	Year	Month	Day	h:min:s	Lat °N	Lon °E	Depth	Mw	Nodal plane 1			Nodal plane 2			*P* axis		*T* axis		Q	CLVD	VR
							km		Strike °	Dip °	Rake °	Strike °	Dip °	Rake °	az °	pl °	az °	pl °		%	%
1	2007	4	09	23:27:15.71	38.539	21.626	15.66	4.4	320	51	−71	111	43	−112	291	75	36	4	A	55	70
2	2007	4	10	00:54:56.35	38.529	21.629	14.91	3.4	327	65	−48	82	48	−145	286	51	28	10	B	5	48
3	**2007**	**4**	**10**	**03:17:56.09**	**38.551**	**21.626**	**14.29**	**5.0**	**325**	**59**	**−72**	**113**	**35**	**−117**	**274**	**70**	**42**	**12**	**A**	**26**	**74**
4	2007	4	10	03:27:38.33	38.534	21.612	5.28	3.9	317	59	−71	103	36	−119	269	70	33	12	C	13	38
5	2007	4	10	03:32:34.20	38.524	21.619	14.15	3.7	296	24	−112	140	68	−80	67	66	223	22	A	51	64
6	2007	4	10	03:39:18.86	38.549	21.663	12.49	3.3	337	61	−50	97	48	−139	299	55	40	7	C	24	31
7	2007	4	10	04:16:15.65	38.550	21.605	2.95	3.1	324	60	−78	121	32	−110	263	72	45	14	C	42	20
8	2007	4	10	04:29:58.11	38.535	21.607	10.96	3.7	320	61	−78	116	31	−111	257	71	41	15	A	23	62
9	2007	4	10	04:47:17.99	38.535	21.622	12.94	3.3	336	32	−71	134	60	−101	16	73	232	14	C	20	27
10	2007	4	10	05:55:12.15	38.531	21.602	9.70	3.1	322	61	−49	81	49	−140	284	54	24	7	B	20	51
11	2007	4	10	06:03:39.12	38.570	21.638	8.54	3.7	327	37	−47	98	64	−117	326	61	207	15	B	5	53
12	2007	4	10	07:13:03.67	38.532	21.651	14.60	4.7	323	66	−63	92	36	−135	273	60	33	16	A	38	70
13	2007	4	10	07:14:12.39	38.567	21.624	12.42	4.4	348	59	−23	90	70	−147	312	37	217	7	A	36	66
14	**2007**	**4**	**10**	**07:15:40.44**	**38.555**	**21.584**	**5.06**	**5.1**	**317**	**60**	**−67**	**97**	**37**	**−124**	**271**	**67**	**31**	**12**	**B**	**28**	**56**
15	2007	4	10	08:13:45.40	38.526	21.614	14.59	3.8	300	32	−84	113	58	−94	12	77	206	13	A	15	61
16	2007	4	10	09:59:01.51	38.560	21.618	11.63	3.5	331	37	−50	105	63	−116	333	63	213	14	B	36	57
17	2007	4	10	10:34:47.97	38.550	21.606	13.62	3.3	320	35	−55	99	62	−112	329	66	205	14	A	53	63
18	**2007**	**4**	**10**	**10:41:00.14**	**38.525**	**21.647**	**22.47**	**5.2**	**325**	**64**	**−65**	**98**	**35**	**−131**	**275**	**62**	**37**	**16**	**A**	**31**	**65**
19	2007	4	10	12:55:17.70	38.539	21.615	12.91	3.3	247	24	−133	113	73	−73	46	59	190	26	C	5	36
20	2007	4	10	13:51:00.93	38.564	21.610	17.81	3.6	341	74	−32	81	59	−161	297	34	34	10	C	9	38
21	2007	4	13	12:58:14.45	38.526	21.616	9.38	3.1	325	60	−42	79	55	−142	290	49	23	3	C	3	38
22	2007	4	15	02:16:32.58	38.574	21.576	17.86	4.1	320	67	−60	84	37	−140	271	57	28	17	A	48	69
23	2007	6	5	11:50:20.46	38.535	21.639	16.57	4.8	339	54	−42	97	57	−136	310	53	217	2	B	23	50
2007 swarm average focal mechanism									325	52	−58	99	48	−124	298	65	33	2			

The strongest events of the swarm are marked in bold.

reported in Delibasis and Carydis (1977). It differs from the composite solution, obtained from first motion polarities of short-period records (Papazachos, 1975), which showed almost pure E–W normal faulting (NP1: strike=98°, dip=59°, rake=−65°, NP2: strike=236°, dip=39°, rake=−125°). To test the validity of a pure normal mechanism we did forward modelling by keeping the focal parameters (strike, dip and rake)

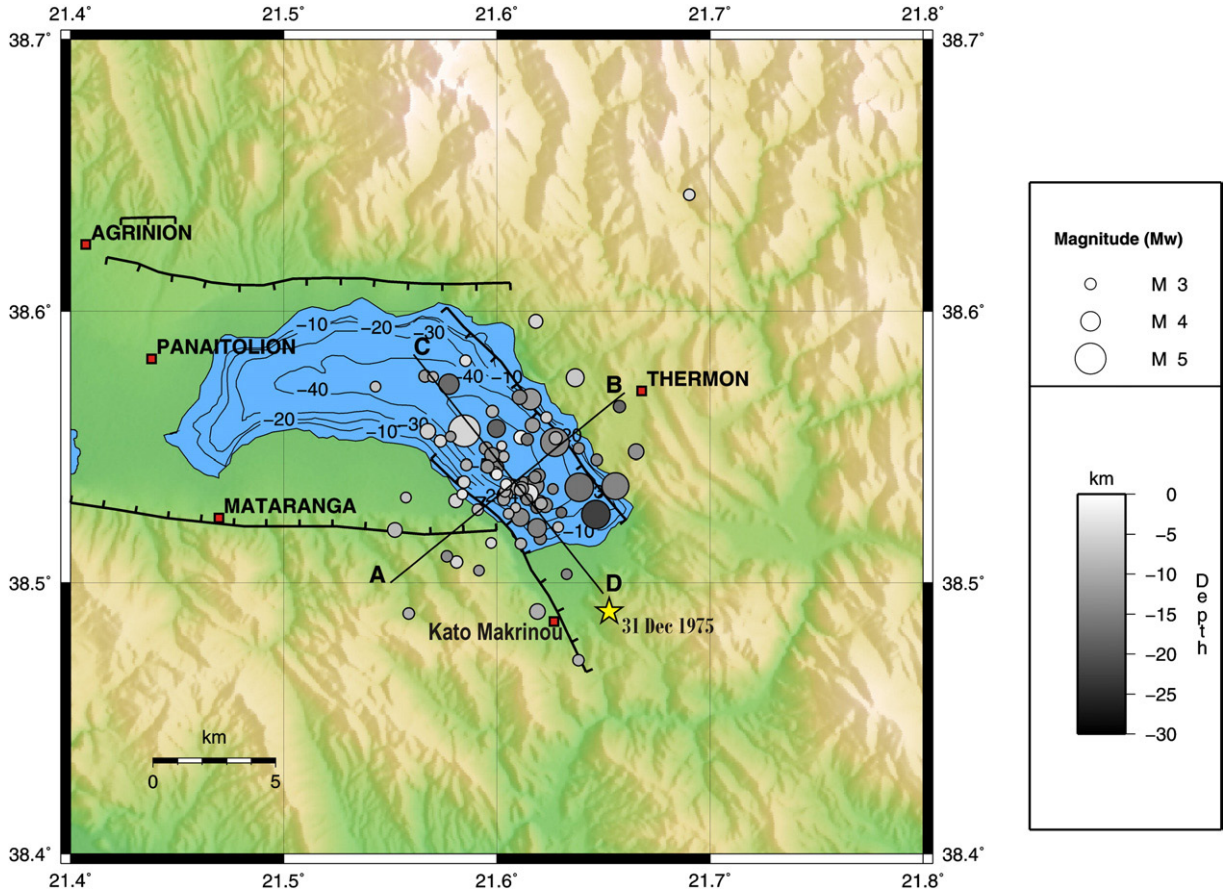

Fig. 6. Distribution of the best located events using Hypoinverse. Earthquake activity is well confined along the two NNW–ESE trending normal faults bounding the eastern banks of Trichonis Lake.

Author's personal copy

fixed, realigning the waveforms if necessary, and inverting for synthetics. The normal faulting solution deteriorates the amplitude fit and predicts reversed polarity, compared to the observed, at three stations (comparison not shown here).

3.2. Relocation of the epicentres of the 1975 events — macroseismic observations

Both the 30 June and 31 December, 1975 events were relocated using Hypoinverse, the velocity model of Haslinger et al. (1999) and the available phases at the International Seismological Centre (ISC). The best solutions (Table 1) place the epicentres near the village of Kato Makrinou, where the maximum intensities (I=VII–VIII and I=IX, respectively) have been reported (ISC — on-line bulletin).

From the two nodal planes of the 31 December 1975 event it is not easy to identify the fault plane. First of all, no aftershock locations are available and only their origin time is provided (Kourouzidis, 2003). Thus, we re-examined the distribution of the reported MM intensities (ISC bulletins and NOA bulletins) for the June–December 1975 strong events, seeking for evidence for the fault plane. We applied the BOXER code (Gasperini et al., 1999; Gasperini and Ferrari, 2000) and the relations of MM to MCS scale (Trifunac and Živčič, 1991) to obtain the macroseismic epicentre and magnitudes, Mw (Table 1). The moment magnitudes for the June and December events, thus obtained, are 5.9 and 5.6, respectively. Based on the same intensity data, the physical dimensions and the orientation of the source (for details see Gasperini et al., 1999) may also be determined. The results indicate an orientation of 137° for the causative fault of the 31 December 1975 event, while for the 30 June 1975 event they indicate an orientation of 112°, suggesting a NW–SE orientation of the causative fault for these events (the sense of dip cannot be determined with this method).

The instrument that recorded both the 30 June and 31 December 1975 events was a SR-100 Wilmot (T=0.75 s, nominal damping=0.10) seismoscope located at the town of Messolongi (38.36°N 21.45°E) approximately 24 km to the SW of the epicentre (Delibasis and Carydis, 1977) and the records shown in Fig. 3 are those as included in the National Observatory of Athens (NOA) monthly bulletins. The 30 June 1975 caused a deflection of 13.6 mm in the N120°E direction and the 31 December 1975 event caused a deflection of 13.5 mm in the ~N130°E direction (Person, 1977). The reported intensities at Messolongi are I=IV–V MM for both events. Using the maximum seismoscope deflections, the characteristics of the Wilmot seismoscope and the formulation of Jennings and Kanamori (1979; Eqs. (14) and (15)) we calculate the corresponding Wood–Anderson amplitude to be ~18.9 m (one-half peak-to-peak) and the resulting ML is of the order of 5.9 for both events. This is contradictory to the fact that the first (June) event has teleseismic waveforms indicating a smaller magnitude compared to the second (December) event, and also to the fact that the raw intensity data as well as the macroseismic moment magnitudes additionally indicate different magnitudes. Unfortunately the seismoscope records cannot resolve the fault plane, as both nodal planes for the December 1975 event predict maximum displacement in the NNW–SSE direction.

Taking into consideration the work of Delibasis and Carydis (1977), who studied in detail the 1975 sequence, the fault structure, our analysis of the macroseismic observations, previous (Brooks et al., 1988; Tselentis, 1998 (especially Fig. 4a)) and recent works (Vött, 2007) we conclude that the June–December 1975 sequence

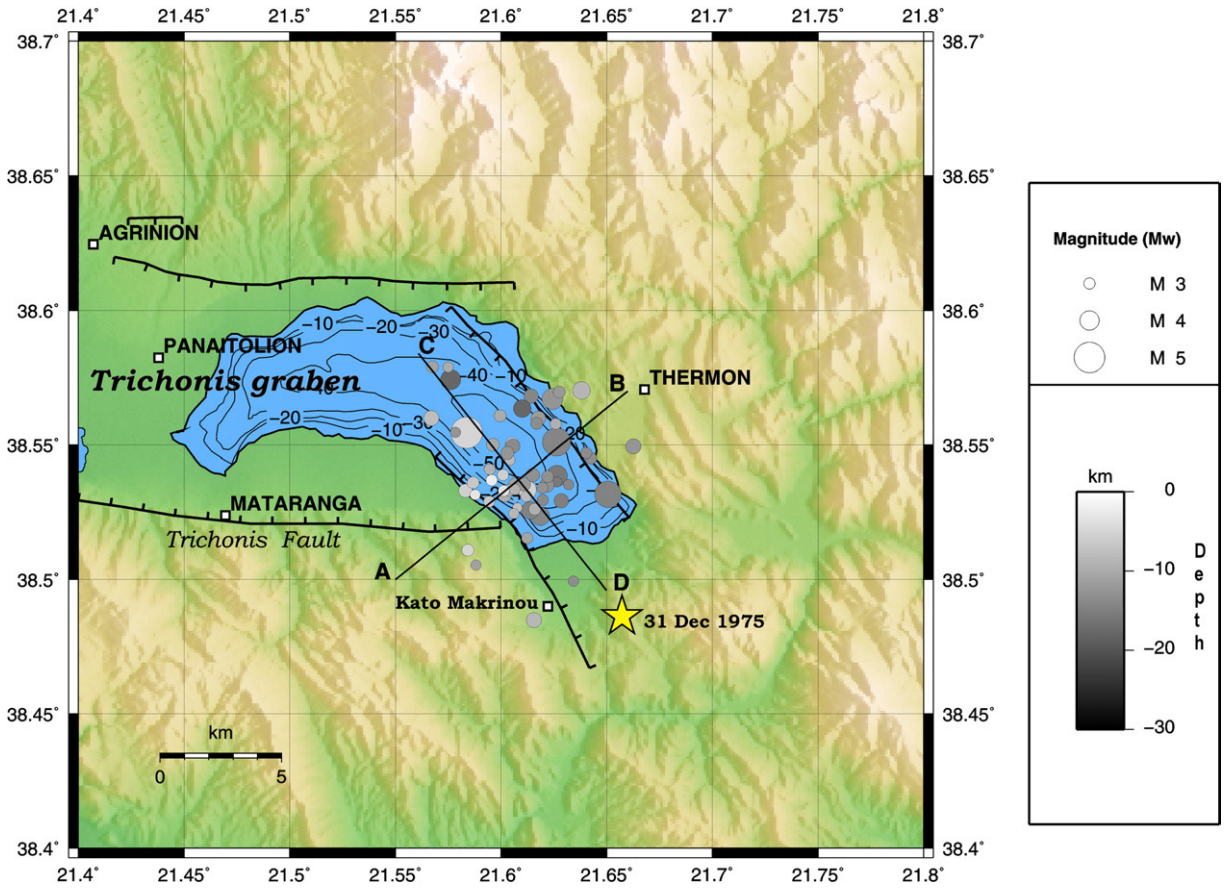

Fig. 7. Our preferred distribution of epicentres using HypoDD and the approach defined in the text. Seismicity is clustering in a NNW–ESE direction, within the eastern part of Lake Trichonis, and is well confined within the two normal faults bounding the banks of the lake. Lines AB and CD define the cross-sections in Fig. 8.

Author's personal copy

was the result of the activation of an NNW–ESE trending normal fault that dips to the NE, with sinistral strike-slip motion. The 2007 swarm exhibited the same pattern as shown later.

4. The April 2007 swarm

4.1. Focal mechanisms of the 2007 swarm

We used moment tensor inversion applied to regional broad-band waveforms to determine the focal mechanisms of twenty-three (23) events of the 2007 swarm. The waveforms were retrieved from the broad-band stations of the Hellenic Unified Seismic Network (Fig. 4). The ISOLA code, (Sokos and Zahradnik, in press) was used to invert the data to retrieve the moment tensor. The method is a modification of the Kikuchi and Kanamori (1991) iterative deconvolution method to regional distances and it includes the computation of the full Green's functions using the discrete wavenumber of Bouchon (1981, 2003). The method allows for multiple source inversion; however for the moderate magnitude events studied here, single source inversion was used. The velocity model of Haslinger et al. (1999) was employed since it was obtained by tomographic investigations in the studied area. The frequency band for the inversion was variable depending on the magnitude of the events; typical values were 0.03 to 0.08 Hz for the strongest events of the swarm and 0.08–0.14 Hz for the moderate magnitude ones. A typical fit for one event (a B solution) is presented (Fig. 5a). The parameters of the focal mechanisms are included in Table 2.

The focal mechanisms of the 2007 swarm (Fig. 5b) indicate normal faulting combined with strike-slip motions, along mainly NNW–SSE trending planes. Only two of the focal mechanisms studied are pure strike-slip. The resulting average mechanism for the 2007 events (using the RAKE software, Louvari and Kiratzi, 1997) has the parameters: Nodal plane 1: strike=325°, dip=52°, rake=−58°; Nodal plane 2: strike=99°, dip=48°, rake=−124°, *T* axis: plunge=2°, trend=N33°E, *P* axis: plunge=65°, trend=N298°E, in accordance with the regional stress field (Kiratzi et al., 1987; Papazachos and Kiratzi, 1996; Papazachos et al., 1998; Kiratzi et al., 2007).

4.2. Distribution of epicentres of the 2007 swarm

We collected all the available phase data (P- and S-wave arrival times) of the recently established in Greece Hellenic Unified Seismic Network (HUSN) and more specifically data from the stations operated by Patras University, Thessaloniki University and the National Observatory of Athens — Geodynamic Institute (Fig. 4) were used, to develop a joint catalogue. From the original data set, we chose only those earthquakes for which 5 or more phases were available. Our final data set consists of 11,798 P- and 5831 S-wave arrival times, corresponding to 79 earthquakes. In all cases we tried to include S arrivals in the closest stations (e.g. SELA, SER, EFP, UPR) to constrain focal depths. For the relocation we used both Hypoinverse (Klein, 2002) and HypoDD (Waldhauser and Ellsworth, 2000) location codes, for reasons of comparison and testing.

4.2.1. Hypoinverse relocation

During trial initial runs several velocity models as well as starting depths were used and the final solutions which have the lowest rms errors are presented in Fig. 6, corresponding to a starting depth of 7 km and the Haslinger et al. (1999) velocity model. In general, we included more than 5 phase readings for each event, and the rms uncertainties ranged from 0.15 to 0.46; mean formal location errors are: rms 0.27 s, ERH 0.71 km and ERZ 2.5 km.

The epicentres are confined in the eastern part of Lake Trichonis, within the two NNW–ESE bounding normal faults (Fig. 6). All events are shallow, confined in the upper 20 km of the crust and the number of events gradually decreases with increasing depth.

4.2.2. HypoDD relocation

Our preferred locations are based on the HypoDD software following the procedure described in Roumelioti et al. (2003). Initial locations (sources) were taken from the derived catalog while stations located within 200 km from the centroid of the initial epicentral area, were used. Thus, 78 initial sources and 15 stations were evolved in the relocation procedure. The double-difference residuals for the pairs of earthquakes at each station were minimized by weighted least squares using the method of singular value decomposition (SVD).

Table 3
Relocated epicentres of the 2007 swarm using HypoDD (see text for details)

No.	Year	Month	Day	Hour	Minute	Second	Lat °N	Lon °E	Depth (km)	Mw
1	2007	4	9	23	27	15.77	38.539	21.626	15.66	4.2
2	2007	4	10	0	6	15.07	38.536	21.626	15.61	2.9
3	2007	4	10	0	8	52.48	38.540	21.614	13.09	2.7
4	2007	4	10	0	54	56.42	38.529	21.629	14.91	3.5
5	2007	4	10	1	48	51.26	38.544	21.604	8.34	2.9
6	2007	4	10	3	17	56.17	38.551	21.626	14.29	4.8
7	2007	4	10	3	27	38.4	38.534	21.612	5.28	3.9
8	2007	4	10	3	32	34.33	38.524	21.619	14.15	3.9
9	2007	4	10	3	39	19.08	38.549	21.663	12.49	3.6
10	2007	4	10	3	43	6.72	38.485	21.616	8.48	3.6
11	2007	4	10	4	16	15.63	38.550	21.605	2.95	3.4
12	2007	4	10	4	29	58.23	38.535	21.607	10.96	3.5
13	2007	4	10	4	47	18.1	38.535	21.622	12.94	3.5
14	2007	4	10	5	20	0.61	38.533	21.583	5.70	3.4
15	2007	4	10	5	39	8.14	38.558	21.626	9.35	3.1
16	2007	4	10	5	55	12.3	38.531	21.602	9.70	3.4
17	2007	4	10	6	3	39.23	38.570	21.638	8.54	3.8
18	2007	4	10	6	16	8.87	38.536	21.587	6.53	3.2
19	2007	4	10	6	19	21.07	38.533	21.604	9.39	3.2
20	2007	4	10	6	32	28.04	38.545	21.643	13.28	3.1
21	2007	4	10	7	5	44.3	38.539	21.601	5.63	3
22	2007	4	10	7	13	3.87	38.532	21.651	14.60	4.7
23	2007	4	10	7	14	12.45	38.567	21.624	12.42	4.2
24	2007	4	10	7	15	40.62	38.555	21.584	5.06	5.1
25	2007	4	10	7	33	7.59	38.535	21.611	11.82	3.4
26	2007	4	10	7	35	26.16	38.560	21.567	7.81	3.6
27	2007	4	10	7	36	57.06	38.511	21.584	4.91	3.2
28	2007	4	10	7	47	32.03	38.550	21.596	10.22	3.3
29	2007	4	10	8	13	45.5	38.526	21.614	14.59	3.8
30	2007	4	10	8	25	17.1	38.527	21.608	7.44	2.8
31	2007	4	10	9	31	7.17	38.537	21.596	2.29	3
32	2007	4	10	9	59	1.57	38.560	21.618	11.63	3.5
33	2007	4	10	10	34	47.96	38.550	21.606	13.62	3.5
34	2007	4	10	11	27	23.5	38.547	21.640	13.45	3.1
35	2007	4	10	11	27	50.7	38.541	21.595	9.03	3
36	2007	4	10	11	29	1.13	38.515	21.612	10.75	3.1
37	2007	4	10	11	40	16.89	38.499	21.634	13.15	2.9
38	2007	4	10	11	51	28.9	38.535	21.632	14.02	2.9
39	2007	4	10	12	14	4.56	38.531	21.612	8.09	3
40	2007	4	10	12	40	4.89	38.534	21.607	9.13	3
41	2007	4	10	12	55	17.83	38.539	21.615	12.91	3.4
42	2007	4	10	13	30	54.09	38.506	21.588	10.95	2.9
43	2007	4	10	13	46	57.4	38.568	21.614	14.13	3.5
44	2007	4	10	13	51	0.94	38.564	21.610	17.81	3.8
45	2007	4	10	16	0	22.63	38.533	21.601	3.52	3
46	2007	4	10	17	55	50.37	38.525	21.606	8.30	2.9
47	2007	4	10	22	59	46.72	38.561	21.600	9.87	3.2
48	2007	4	10	23	32	14.05	38.529	21.595	6.42	3.1
49	2007	4	10	23	59	17.22	38.555	21.578	12.45	2.9
50	2007	4	11	0	56	32.62	38.530	21.620	13.71	3.1
51	2007	4	11	3	39	36.49	38.558	21.617	13.35	3.2
52	2007	4	11	6	6	32.38	38.579	21.568	10.82	3.2
53	2007	4	11	7	45	9.26	38.570	21.628	12.03	3.2
54	2007	4	11	20	6	1.07	38.538	21.622	12.95	3.2
55	2007	4	11	20	13	13.65	38.534	21.620	12.65	3.1
56	2007	4	12	10	32	56.08	38.532	21.588	3.01	2.9
57	2007	4	12	14	32	49.04	38.547	21.603	12.36	3.3
58	2007	4	13	12	58	14.56	38.526	21.616	9.38	3.2
59	2007	4	15	2	16	32.54	38.574	21.576	17.86	4.1
60	2007	4	15	3	12	35.11	38.579	21.575	9.78	2.9

Author's personal copy

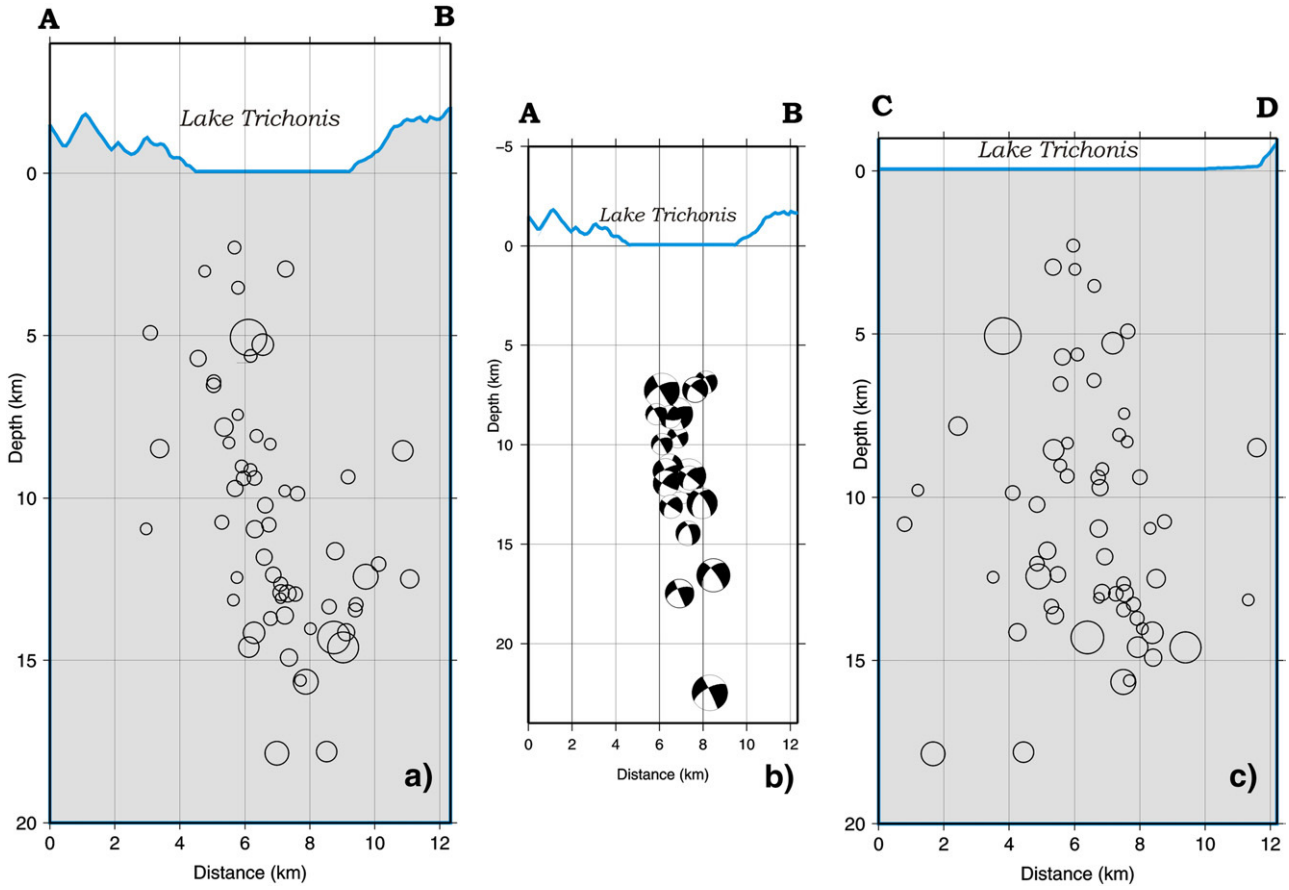

Fig. 8. Cross-sections a) along dip (section AB in Fig. 7) and c) along strike (section CD in Fig. 7) to show the confinement of epicentres within the banks of Lake Trichonis, the dip of the fault plane at ~70°–80° to NE, and the depth distribution of the swarm hypocentres to the upper 15 km of the crust. Topography is shown for comparison; b) cross-section along AB and projection of the focal mechanisms to confirm the sense and steepness of dip angles.

Since we were dealing with a small number of events, we selected value 1 for minimum number of observations at each event pair and the number of stations (15) for maximum number of observations at each event pair. The maximum number of neighbouring events was set to the number of the initial sources. Theoretical travel-time differences were estimated based on the 1D P-velocity model (Haslinger et al., 1999) and S-wave velocities were estimated from this model, assuming a V_P/V_S ratio of 1.78 (Kiratzi et al., 1987; Tselentis et al., 1996).

The HypoDD final results include 77% of the sources included in the initial data set (60 relocated events show a spatial pattern more compact compared to previous solutions). The relocated hypocentres (Fig. 7) are clustered mainly at the eastern part of the lake, the centroid of which is defined at Lat: 38.5409° N, Lon: 21.6097° E and at a depth of 10.6 km. The average uncertainties in our locations are: 0.10 km in the E–W direction, 0.05 km in the N–S direction and 0.23 km in the vertical direction, and the rms residual is 8.1 ms. The distribution of epicentres (Table 3 and Fig. 7) is mainly confined within the eastern banks of the lake, reach depths up to 17 km and the strongest events of the swarm are aligned along a NNW–ESE direction, in accordance with the average focal mechanism, previously mentioned, specifically with the nodal plane that strikes at N325°. The dimensions of this earthquake cluster are approximately 6 km×4 km, along strike and along dip, respectively, in accordance with scaling relations for a class M5.2 event (Wells and Coppersmith, 1994).

Fig. 8 presents cross-sections of aftershocks and of focal mechanisms along dip (AB) and along strike (CD) (see also Fig. 7), which indicate: a) steep dip angle of the fault plane (~70°–80°) towards NE, steeper than the dip angle obtained from the 2007 swarm focal mechanisms, in accordance though with the dip angle (71°) of the 31 Dec 1975 event; b) confinement of earthquake activity in the upper 15 km of the crust and c) evidence for activation of the antithetic fault of the lake, that dips to SW.

5. Stress transfer related to the 1975 event

To model the changes on the stress field after the occurrence of the 31 December 1975 event, using Coulomb stress modelling (Reasenberg and Simpson, 1992; Harris and Simpson, 1992), we used the program DLC, written by R. Simpson, based on the subroutines of Okada (1992), assuming elastic rheology (Coulomb failure function or CFF) and static effects. All calculations assumed a Poisson's ratio of 0.25 and a shear modulus of 300,000 bar (30 GPa).

First the stress field due to the Dec 1975 event was calculated using the parameters of Table 1 and assuming a 10 km long and a 8 km wide rupture that satisfies the empirical requirements for a Mw=6.0 magnitude earthquake (Wells and Coppersmith, 1994). Then we computed the static stress changes on average fault planes of the 2007 sequence (Fig. 5) i.e. N325°E strike, 52° dip to NE and −58° rake. Several runs at various depths in the upper crust were performed and we present here the map of Coulomb stress change for the depth of 10.6 km (Fig. 9), the average depth of the 2007 swarm as shown by the HypoDD procedure (Table 3). Positive stress change (red colours) indicates that slip along receiver faults is encouraged or triggered while negative (blue) change indicates that slip is discouraged or delayed (Fig. 9). We also tested a range of values for the effective coefficient of friction (μ') along the receiver faults and we adopted a value of 0.4 which is considered an average value for regions

Author's personal copy

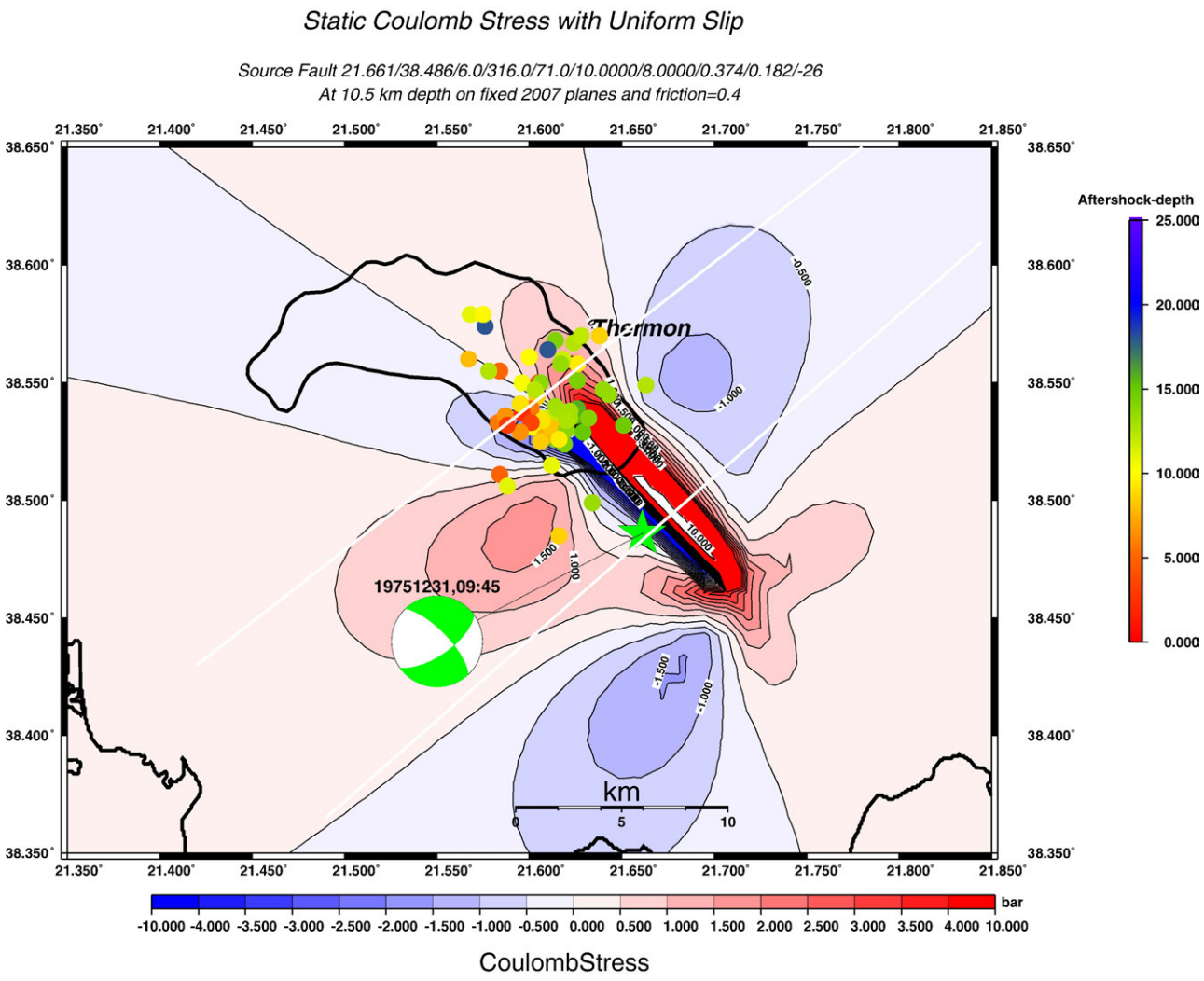

Fig. 9. Map of Coulomb stress changes in the vicinity of the 31 Dec 1975 rupture (Mw=6.0). The map shows loaded (red) areas and relaxed (blue) areas at a depth of 10.5 km (average depth of 2007 sequence). Stress calculations are valid for the average slip model of the 2007 sequence (fixed planes). Beach ball indicates focal mechanism of the 1975 event and small circles indicate epicentres of the 2007 swarm (colours correspond to different depths). Scale is in bar.

containing both mature and minor faults (Parsons et al., 1999). A higher value such as 0.8 gave results with increased levels of Coulomb stress, (ΔCFF) as it is a linear function of the form $\Delta CFF = \Delta\tau + \mu'\Delta\sigma_n$ (where $\Delta\tau$ is the change in shear stress resolved along the receiver fault and $\Delta\sigma_n$ is the change in the normal stress acting across the fault plane). As we defined the end of the 1975 rupture at −8 km the Coulomb stress map shows a large load of stress on rocks and fault planes on mid-crust levels (10.5 km; Fig. 9) exceeding 4 bar (0.4 MPa). The 2007 swarm is entirely located to the NW of the 1975 epicentre and outside its rupture plane. We suggest that the majority of the epicentres deeper than 10 km are located in the loaded region and could have been triggered because Coulomb stress levels range from +0.5–4.1 bar (Fig. 9). In particular, the 20070410, 03:17 event that was third in the sequence with a moment magnitude of 5.0 is located in the loaded region.

To investigate the triggering relation graphically we present two cross-sections of ΔCFF in the direction N46E, i.e. normal to the strike of the 1975 rupture plane and also normal to the average strike of the modelled receiver faults (N325°E; Fig. 10). On the same sections one can also see the projections of the April 2007 swarm hypocentres (green dots). The section going through the 1975 hypocentre shows a broad relaxed region exceeding up to 20 km on either side of the rupture and directed NE–SW (Fig. 10a). However, large ΔCFF levels are observed near the surface (0–3 km) and near the bottom of the fault plane and further down-dip until the depth of 15+ km where they reach 0.5 bar. The post-1975 seismicity (Fig. 1) shows no large earthquakes along NW–SE directed fault planes (or other orientations) so we infer that the stress modelling shown in Fig. 10a is correct. We note that similar stress shadows such as those produced by the 1975 events have been observed in the Atalanti region, central Greece, after a double event in April 1894 (Ganas et al., 2006) and their existence influences seismicity rates (Harris and Simpson, 1996). In addition, the NE–SW cross-section at the middle of the 2007 swarm area (Fig. 10b; 7 km to the NW of the 1975 epicentre) shows that a broad zone (the red "channel") of increased ΔCFF has developed with values exceeding 4 bar between 5 and 10 km depth. This zone is about 2.5 km wide and dips steeply to the NE. It is located at the NW termination of the 1975 rupture. The projection of the 2007 epicentres on this cross-section shows that the majority of the events fall inside this channel of increased ΔCFF. We infer that the occurrence of the 2007 events has been enhanced by stress transfer due to the 1975 mainshock.

6. The left-lateral shear north of the Gulf of Corinth

The 2007 earthquake swarm together with the processing of the 1975 teleseismic data provided new insights into the seismotectonics

Author's personal copy

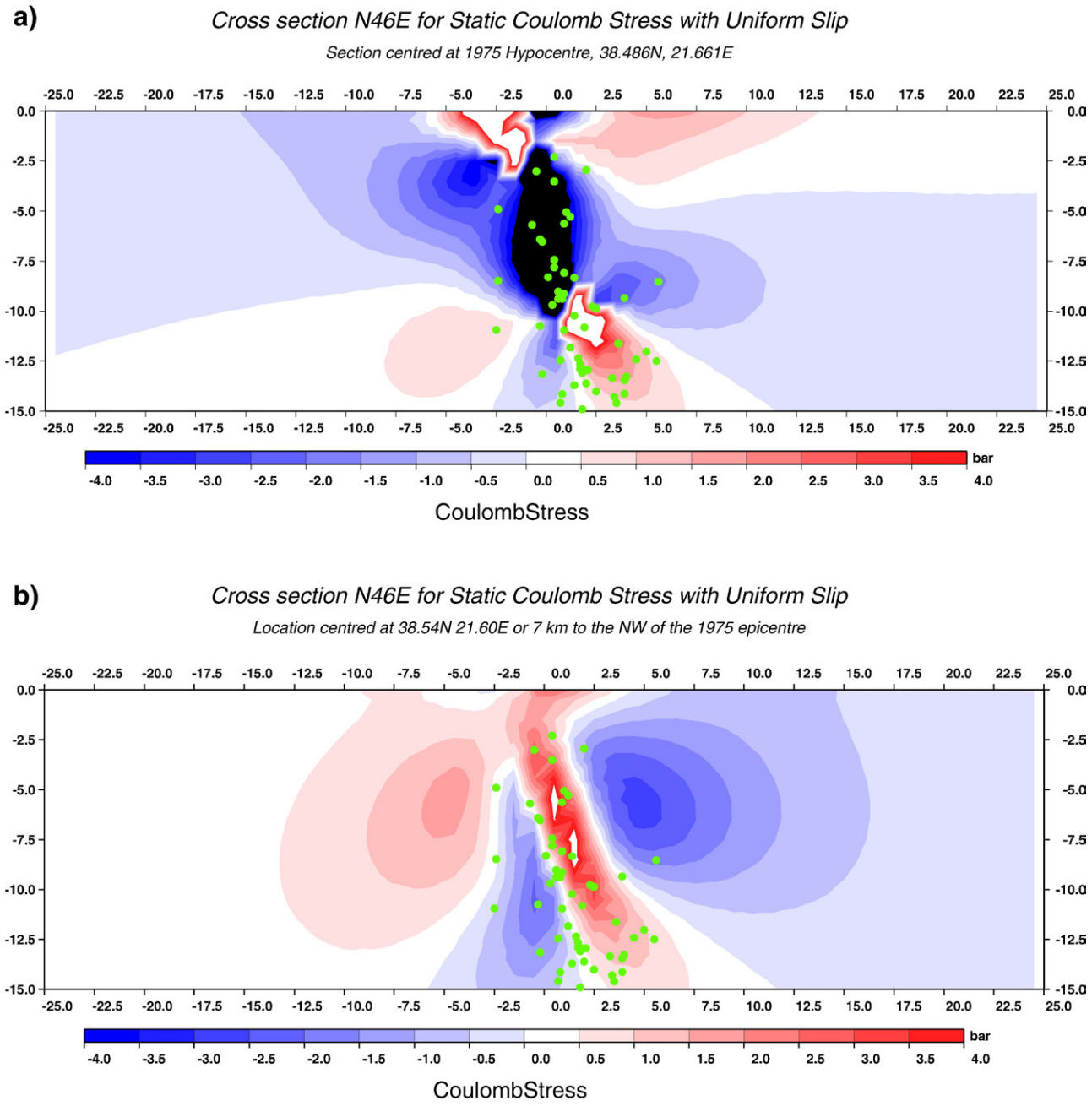

Fig. 10. Vertical cross-sections of Coulomb stress change (ΔCFF) through the upper crust with orientations N46°E (i.e. normal to the 1975 rupture plane); a) section centred at the 1975 hypocentre showing broad relaxation along the rupture plane and stress transfer towards the top and the bottom of the rupture; b) section located 7 km to the NW of the 1975 event (axes in km) showing the stress transfer geometry (high-angle red channel) at the NW termination of the 1975 rupture. Green dots are projected hypocentres of the 2007 swarm. Scale is in bar. Both sections are shown as thin white lines on Fig. 9.

of this region. The new key elements are (Fig. 11): a) the NW–SE strike of the activated fault zone during both the 1975 shallow events and the 2007 swarm b) that those earthquakes did not rupture the Trichonis fault (Fig. 1), which is the most prominent tectonic feature in the region, but they ruptured the NW–SE trending normal fault that bounds the south-eastern bank of the lake and dips to the NE; and c) the left-lateral component of the motion that was mapped throughout the sequence. We suggest that this tectonic setting is due to the activation of a left-lateral, crustal-scale shear zone, about 25 km long. The shear zone links two right-stepping juvenile rifts, the Trichonis and the Corinth graben, respectively (Fig. 11). Ignoring local complexities and minor antithetic faulting the finite extension of the crust in the N–S direction creates a left-lateral simple shear of the upper crust in the tip region between the two grabens (Fig. 11 inset). Our seismological data are better interpreted by the activation of such a shear zone than some type of "diffused" deformation between en-echelon rift segments. The southern termination of this left-lateral shear zone may be found in the broader Nafpaktos area (Fig. 11). Indeed, the Nafpaktos area is a relatively low-slip area in comparison to the south coast of the Gulf of Corinth where several north-dipping normal faults are active (Houghton et al., 2003; Palyvos et al., 2005; Bernard et al., 2006).

Our model is developed in Fig. 11 where the long, N–S arrows indicate regional (far-field) extension direction while arrow marked with τ_{max} indicates the resolved shear stress that drives seismic slip along the NW–SE discontinuity. It is possible to drive shear along this fault zone if we assume that locally the stress field has rotated at 45° to

Author's personal copy

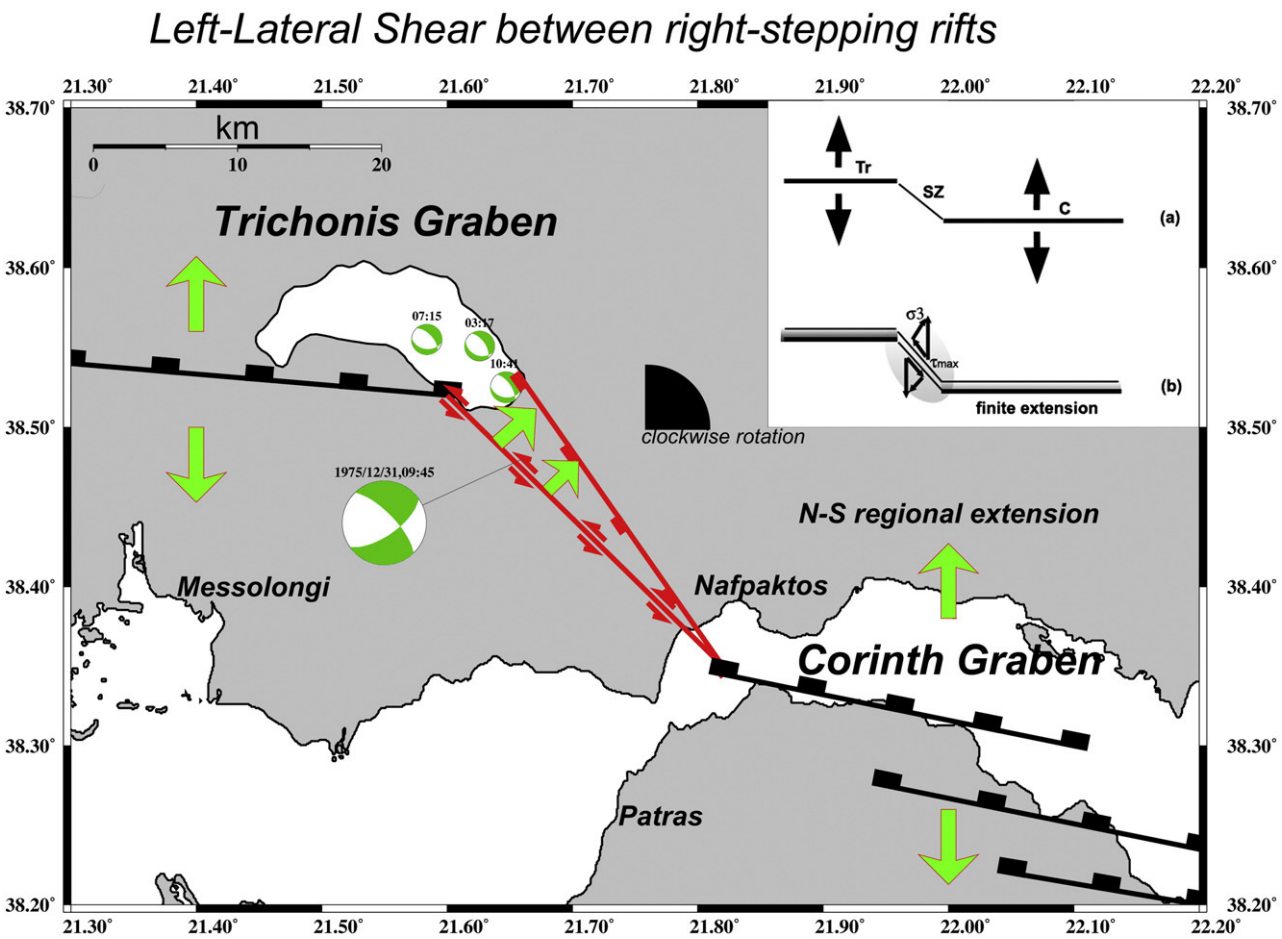

Fig. 11. Map of western Greece showing the structural relationship of the two sub-parallels, E–W striking Quaternary Grabens (Corinth and Trichonis) and the origin of the left-lateral shear along the NW–SE direction between Nafpaktos and Lake Trichonis. Inset sketch shows the development of simple shear deformation between two non-overlapping rifts where σ_3 denotes local minimum compressional stress direction and τ_{max} plane of maximum shear stress. We propose a 25 km left-lateral shear zone striking NW–SE between the two rifts dipping at a high-angle to the NE. Deformation is dominated by normal faulting because of large, differential rotations of crustal blocks on either side of the Gulf of Corinth that locally create NE–SW extension. Beach balls indicate focal mechanisms of the 31 December 1975 and the three stronger 2007 events (compressional quadrants shaded).

the orientation of the structure (Scholz, 2002, p. 142). We suggest that inside this zone the azimuth of the maximum compressional stress (σ_1) is provided by the orientation of the *P* axis of the earthquakes that we studied (i.e. E–W to SE–NW; Tables 1 and 2). This model is compatible with the N–S directed, far-field extension.

The normal component of the deformation originates from finite strain constraints, i.e. from spreading (new space) that is created due to the clockwise (vertical-axis) rotation of the crustal block to the north of the Gulf of Corinth (Fig. 11; Avallone et al., 2004). The creation of new space is due to the increasing rotation rate from south (2.8° per My) to north (7° per My) as evidenced by the GPS data of Avallone et al. (2004). This "spreading" effect is normal to the trend of the shear zone; however, we note that this local extension is a secondary effect within the prevailing N–S extension since no field evidence exists for a major strike-slip zone in this area, except for the NW–SE orientation of the lake's coastline near the 2007 swarm epicentres. In the elastic upper crust this spreading is accommodated by slip along normal faults such as the fault that ruptured during the 1975 earthquake and the faults activated during the 2007 swarm. Therefore the model (Fig. 11, inset) includes a small NE–SW arrow marked with σ_3 which indicates the local extension direction as obtained from the average *T*-axis plunge and plunge direction in Table 2. This process resembles the extension created at releasing bends of major strike-slip faults known as "pull-apart", only that in the Trichonis case the releasing factor is the differential clockwise rotation of crustal blocks. As previously mentioned such clockwise rotations are well documented elsewhere in western Greece from paleomagnetic data (van Hinsbergen et al., 2005, 2006; Vött, 2007). The block rotations are necessary to accommodate large scale deformation of the Hellenic Arc due to a combination of motions from the N215°E-advancing Aegean microplate over the N5°W-moving Nubia plate (Goldsworthy et al., 2002; Fernandes et al., 2003). Another implication of this tectonic model is that the Trichonis graben cannot grow towards the east so the size of future, strong earthquakes along the lake's south coast can be better constrained.

In summary, our study substantiates the existence of a significant strike-slip component in the active tectonics to the NW of the Gulf of Corinth. Previous studies in this region of western Greece (Hatzfeld et al., 1988; Baker et al., 1997) showed primarily normal or thrust faulting. Hatzfeld et al. (1988) reported two small events with *P* axes trending NW–SE to the east of lake Trichonis but without further discussion. However, strike-slip motions have been recorded inside the Gulf of Patras during the 1993 earthquake sequence (Ms=5.4; Tselentis et al., 1994; Tselentis, 1998; Kiratzi and Louvari, 2003) where the NW–SE alignment of aftershocks points to the activation of a left-lateral strike-slip fault. The along-strike extent of the 1993 aftershocks reached 25 km in the NW–SE direction cutting through the eastern part of the Gulf. The Gulf of Patras is a well-studied Quaternary Graben where the main structure is north-dipping (Ferentinos et al., 1985; Chronis et al., 1991). This configuration of active structures resembles closely the Trichonis graben in the sense that both grabens show asymmetry (southern faults are more active) and terminate against NW–SE left-lateral faults.

Author's personal copy

7. Conclusions

The April 2007 earthquake swarm that occurred in Lake Trichonis provided high quality digital data, to the recently established Hellenic Unified Seismograph Network (HUSN), which we used to relocate epicentres and determine focal mechanisms. The epicentres of 2007 swarm are confined within the eastern shores of the lake – bounded by two NNW–ESE trending normal faults – and in close proximity to the epicentres of the June–December 1975 earthquake sequence, the strongest instrumentally recorded events affecting the region of this study. The majority of those have occurred inside a high-angle "channel" of increased Coulomb stress (Fig. 10) that extends beneath the lake up to mid-crustal levels as a result of the 31 December 1975 earthquake. We applied teleseismic waveform inversion to obtain the focal mechanism of the 31 December 1975 event, and the results show that it was produced by normal faulting along a NNW–ESE striking fault (N316°E), combined with considerable sinistral strike-slip component. The focal mechanisms for 23 events of the 2007 swarm also clearly imply normal faulting along NNW–ESE trending planes, sometimes exhibiting an amount of left-lateral motion.

The 2007 earthquake swarm gave us new insights into the seismotectonics of this region. The new key elements are: a) the NW–SE strike of the activated fault zone, i.e. the 1975 events and the 2007 swarm did not rupture the south Trichonis fault, which is the most prominent tectonic feature in the region, but they ruptured the NW–SE trending normal fault that bounds the south-eastern bank of the lake and dips to the NE; and b) the left-lateral component of the slip vector that was mapped throughout the sequence. We suggest that this tectonic setting is due to the combination of "spreading" due to vertical-axis rotation of crustal blocks and to left-lateral, crustal-scale shear that links two right-stepping normal fault zones, the Trichonis and the Corinth graben, respectively (Fig. 11).

Acknowledgments

We acknowledge (A.K., C.B and Z.R) with thanks financial support from the General Secretariat of Research and Technology (Ministry of Development — Greece), and from INTERREG IIIA (Greece-Fyrom). We also thank G. Stavrakakis, the Director of the Geodynamic Institute of Athens, for providing phase data. AG thanks Bob Simpson and Tom Parsons for discussions on stress transfer. Two anonymous reviewers are also thanked for constructive suggestions. Most of the figures were produced using the GMT software (Wessel and Smith, 1998).

References

Ambraseys, N., 2001a. Reassessment of earthquakes, 1900–1999, in the Eastern Mediterranean and the Middle East. Geophys. J. Int. 145, 471–485.
Ambraseys, N., 2001b. Assessment of surface wave magnitudes of earthquakes in Greece. J. Seismol. 5, 103–116.
Avallone, A., Briole, P., Balodimou, A., Billiris, H., Charade, O., Mitsakaki, X., Nercessian, A., Papazissi, K., Paradissis, D., Veis, G., 2004. Analysis of eleven years of deformation measured by GPS in the Corinth Rift Laboratory area. C. R. Geosciences 336, 301–311.
Baker, C., Hatzfeld, D., Lyon-Caen, H., Papadimitriou, E., Rigo, A., 1997. Earthquake mechanisms of the Adriatic Sea and Western Greece: implications for the oceanic subduction-continental collision transition. Geophys. J. Int. 131, 559–594.
Benetatos, C., Kiratzi, A., Papazachos, C., Karakaisis, G., 2004. Focal mechanisms of shallow and intermediate depth earthquakes along the Hellenic Arc. J. Geodyn. 37, 253–296.
Benetatos, C., Kiratzi, A., Roumelioti, Z., Stavrakakis, G., Drakatos, G., Latoussakis, I., 2005. The 14 August 2003 Lefkada Island (Greece) earthquake: focal mechanisms of the mainshock and of the aftershock sequence. J. Seismol. 9, 171–190.
Bernard, P.H., Lyon-Caen, P., Briole, A., Deschamps, F., Boudin, K., Makropoulos, P., Papadimitriou, F., Lemeille, G., Patau, H., Billiris, D., Paradissis, K., Papazissi, H., Castarède, O., Charade, A., Nercessian, A., Avallone, F., Pacchiani, J., Zahradnik, S., Sacks Linde, A., 2006. Seismicity, deformation and seismic hazard in the western rift of Corinth: new insights from the Corinth Rift Laboratory (CRL). Tectonophysics 426, 7–30.
British Petroleum Co. Ltd, 1971. The geological results of petroleum exploration in western Greece. Geology of Greece, vol. 10. IGSR (now IGME), Athens.
Brooks, M., Ferentinos, G., 1984. Tectonics and sedimentation in the Gulf of Corinth and the Zakynthos and Kefallinia Channels, Western Greece. Tectonophysics 101, 25–54.
Brooks, M., Clews, J., Melis, N., 1988. Structural development of Neogene basins in western Greece. Basin Res. 1, 129–138.
Bouchon, M., 1981. A simple method to calculate Green's functions for elastic layered media. Bull. Seismol. Soc. Am. 71, 959–971.
Bouchon, M., 2003. A review of the discrete wavenumber method. Pure Appl. Geophys. 160, 445–465.
Chronis, G., Piper, D., Anagnostou, C., 1991. Late Quaternary evolution of the Gulf of Patras, Greece: tectonism, deltaic sedimentation and sea-level change. Mar. Geol. 97 (1–2), 191–209.
Delibasis, N., Carydis, P., 1977. Recent earthquake activity in Trichonis region and its tectonic significance. Ann. Geofis. 30, 19–81.
Doutsos, T., Kontopoulos, N., Frydas, D., 1987. Neotectonic evolution of northwestern-continental Greece. Geol. Rundsch. 76, 433–450.
Doutsos, T., Kontopoulos, N., Poulimenos, G., 1988. The Corinth–Patras rift as the initial stage of continental fragmentation behind an active island arc (Greece). Basin Res. 1, 177–190.
Ferentinos, G., Brooks, M., Doutsos, T., 1985. Quaternary tectonics in the Gulf of Patras, western Greece. J. Struct. Geol. 7, 713–717.
Fernandes, R., Ambrosius, B., Noomen, R., Bastos, L., Wortel, M., Spakman, W., Govers, R., 2003. The relative motion between Africa and Eurasia as derived from ITRF2000 and GPS data. Geophys. Res. Lett. 30, 1828. doi:10.1029/2003GL017089.
Ganas, A., Sokos, E., Agalos, A., Leontakianakos, G., Pavlides, S., 2006. Coulomb stress triggering of earthquakes along the Atalanti Fault, central Greece: two April 1894 M6+ events and stress change patterns. Tectonophysics 420, 357–369.
Gasperini, P., Ferrari, G., 2000. Deriving numerical estimates from descriptive information: the computation of earthquake parameters. Ann. Geofis. 43, 729–746.
Gasperini, P., Bernardini, F., Valensise, G., Boschi, E., 1999. Defining seismogenic sources from historical earthquake felt reports. Bull. Seismol. Soc. Am. 89, 94–110.
Goldsworthy, M., Jackson, J., Haines, J., 2002. The continuity of active fault systems in Greece. Geophys. J. Int. 148, 596–618.
Harris, R.A., Simpson, R.W., 1992. Changes in static stress on southern California faults after the 1992 Landers earthquake. Nature 360, 251–254.
Harris, R.A., Simpson, R.W., 1996. In the shadow of 1857 — the effect of the great Ft. Tejon earthquake on subsequent earthquakes in southern California. Geophys. Res. Lett. 23, 229–232.
Haslinger, F., Kissling, E., Ansorge, J., Hatzfeld, D., Papadimitriou, E., Karakostas, V., Makropoulos, K., Kahle, H.G., Peter, Y., 1999. 3D crustal structure from local earthquake tomography around the Gulf of Arta (Ionian region, NW Greece). Tectonophysics 304, 201–218.
Hatzfeld, D., Pedotti, G., Hatzidimitriou, P., Makropoulos, K., 1988. The strain pattern in the western Hellenic Arc deduced from a microearthquake survey. Geophys. J. Int. 101, 181–202.
Hatzfeld, D., Kassaras, I., Panagiotopoulos, D.G., Amorese, D., Makropoulos, K., Karakaisis, G.F., Coutant, O., 1995. Microseismicity and strain pattern in North-western Greece. Tectonics 14, 773–785.
Houghton, S.L., Roberts, G.P., Papanikolaou, I.D., McArthur, J.M., Gilmour, M.A., 2003. New ^{234}U–^{230}Th coral dates from the western Gulf of Corinth: implications for extensional tectonics. Geophys. Res. Lett. 30 (19), 2013. doi:10.1029/2003GL018112.
Jennings, P.C., Kanamori, H., 1979. Determination of local magnitude ML, from seismoscope records. Bull. Seismol. Soc. Am. 69, 1267–1288.
Kokkalas, S., Xypolias, P., Koukouvelas, I., Doutsos, T., 2006. Postcollisional contractional and extensional deformation in the Aegean region. Geol. Soc. Amer. Bull. 409, 97–123 Special Paper.
Kikuchi, M., Kanamori, H., 1991. Inversion of complex body waves—III. Bull. Seismol. Soc. Am. 81, 2335–2350.
Kiratzi, A., Louvari, E., 2003. Focal mechanisms of shallow earthquakes in the Aegean Sea and the surrounding lands determined by waveform modeling: a new database. J. Geodyn. 36, 251–274.
Kiratzi, A., Papadimitriou, E., Papazachos, B., 1987. A microearthquake survey in the Steno dam site in northwestern Greece. Ann. Geophys. 592, 161–166.
Kiratzi, A., Benetatos, C., Roumelioti, Z., 2007. Distributed earthquake focal mechanisms in the Aegean Sea. Bull. Geol. Soc. Greece, 1125–1137.
Klein, F.W., 2002. User's guide to HYPOINVERSE-2000, a FORTRAN program to solve earthquake locations and magnitudes. U. S. Geological Survey Open File Report 02-171 Version 1.0.
Kourouzidis, M.C., 2003. Study of seismic sequences in Greece and its contribution to earthquake prediction. Ph.D. Thesis, Univ. Thessaloniki, 150pp. (in Greek, with an English abstract).
Lekkas, E., Papanikolaou, D., 1997. Neotectonic Map of Greece, Aitolia-Akarnania sheet (scale 1:100.000). Applied Scientific Program, University of Athens, Dept of Dynamic, Tectonic and Applied Geology, Technical report, 148pp. (In Greek).
Louvari, E., Kiratzi, A., 1997. Rake: a windows program to plot earthquake focal mechanisms and stress orientation. Comp. Geosci. 23, 851–857.
Melis, N.S., Brooks, M., Pearce, R.G., 1989. A microearthquake study in the Gulf of Patras region, western Greece, and its seismotectonic interpretation. Geophys. J. Int. 98, 515–524.
Okada, Y., 1992. Internal deformation due to shear and tensile faults in a half-space. Bull. Seismol. Soc. Am. 82, 1018–1040.
Palyvos, N., Pantosti, D., De Martini, P.M., Lemeille, F., Sorel, D., Pavlopoulos, K., 2005. The Aigion–Neos Erineos coastal normal fault system (western Corinth Gulf Rift, Greece): geomorphological signature, recent earthquake history, and evolution. J. Geophys. Res. 110, B09302. doi:10.1029/2004JB003165.
Papadopoulos, G.A., Plessa, A., 2000. Magnitude–distance relations for earthquake-induced landslides in Greece. Eng. Geol. 58, 377–386.
Papazachos, B., 1975. Seismic Activity Along the Saronikos–Corinth–Patras Gulfs. National Observatory of Athens, Geodynamic Institute. Monthly Bulletin April 1975, 9 pp.

Author's personal copy

Papazachos, C., Kiratzi, A., 1996. A detailed study of the active crustal deformation in the Aegean and surrounding area. Tectonophysics 253, 129–154.
Papazachos, B., Papazachou, C., 2003. Earthquakes of Greece, 3rd edition. Ziti Publications, Thessaloniki. 286 pp.
Papazachos, B., Papaioannou, C., Papazachos, C., Savvaidis, A., 1997. Atlas of Isoseismal Maps for Strong Shallow Earthquakes in Greece and Surrounding Area (426 BC–1995). Publication No. 4. Geophys. Lab., Univ. of Thessaloniki. 176 pp.
Papazachos, B.C., Papadimitriou, E.E., Kiratzi, A.A., Papazachos, C.B., Louvari, E.K., 1998. Fault plane solutions in the Aegean Sea and the surrounding area and their tectonic implication. Boll. Geofis. Teor. Appl. 39, 199–218.
Parsons, T., Stein, R.S., Simpson, R.W., Reasenberg, P.A., 1999. Stress sensitivity of fault seismicity: a comparison between limited-offset oblique and major strike-slip faults. J. Geophys. Res. 104, 20183–20202.
Person, W., 1977. Seismological notes — May–December 1975. Bull. Seismol. Soc. Am. 67, 1225–1238.
Reasenberg, P.A., Simpson, R., 1992. Response of regional seismicity to the static stress change produced by the Loma Prieta earthquake. Science 255, 1687–1690.
Roumelioti, Z., Kiratzi, A., Melis, N., 2003. Relocation of the July 26, 2001 Skyros Island (Greece) earthquake sequence using the double-difference technique. Phys. Earth Planet Inter. 138, 231–239.
Roumelioti, Z., Ganas, A., Sokos, E., Petrou, P., Serpetsidaki, A., Drakatos, G., 2007. Toward a joint catalogue of recent seismicity in western Greece: preliminary results. Bull. Geol. Soc. Greece 40, 1257–1266.
Scholz, C., 2002. The Mechanics of Earthquakes and Faulting, 2nd ed. Cambridge University Press, Cambridge. 471 pp.
Sokos, E., Zahradnik, J., in press. ISOLA a Fortran code and a Matlab GUI to perform multiple-point source inversion of seismic data. Comp. Geosci. doi:10.1016/j.cageo.2007.07.005
Trifunac, M.D., Živčić, M., 1991. A note on instrumental comparison of the Modified Mercalli Intensity (MMI) in the western United States and the Mercalli–Cancani–Sieberg (MCS) intensity in Yugoslavia. Eur. Earthq. Eng. 1, 22–26.
Tselentis, G.-A., 1998. Fault lengths during the Patras 1993 earthquake sequence as estimated from the pulse width of initial P-wave. Pure Appl. Geophys. 152, 75–89.
Tselentis, G., Melis, N., Sokos, E., 1994. The Patras (July 14, 1993; Ms=5.4) earthquake sequence. Bull. Geol. Soc. Greece 30, 159–165.
Tselentis, G.-A., Melis, N., Sokos, E., Papatsimpa, K., 1996. The Egion June 15, 1995 (6.2 ML) earthquake, Western Greece. Pure Appl. Geophys. 147, 83–98.
van Hinsbergen, D.J.J., Langereis, C.G., Meulenkamp, J.E., 2005. Revision of the timing, magnitude and distribution of Neogene rotations in the western Aegean region. Tectonophysics 396, 1–34.
van Hinsbergen, D.J.J., van der Meer, D.G., Zachariasse, W.J., Meulenkamp, J.E., 2006. Deformation of western Greece during Neogene clockwise rotation and collision with Apulia. Int. J. Earth Sci. 95, 463–490.
Vött, A., 2007. Relative sea level changes and regional tectonic evolution of seven coastal areas in NW Greece since the mid-Holocene. Quat. Sci. Rev. 26, 894–919.
Waldhauser, F., Ellsworth, W.L., 2000. A double-difference earthquake location algorithm: method and application to the Northern Hayward fault, California. Bull. Seismol. Soc. Am. 90, 1353–1368.
Wells, D.L., Coppersmith, K.J., 1994. New empirical relationships among magnitude, rupture length, rupture width, rupture area, and surface displacement. Bull. Seismol. Soc. Am. 84, 974–1002.
Wessel, P., Smith, W.H.F., 1998. New improved version of the Generic Mapping Tools released. EOS Trans. AGU 79, 579.
Zacharias, I., Dimitriou, E., Koussouris, T., 2005. Integrated water management scenarios for wetland protection: application to Trichonis Lake. Environ. Model. Softw. 20, 177–185.
Zwick, P., McCaffrey, R., Abers, G., 1994. MT5 Program, IASPEI Software Library, p. 4.